



## COMPARISON OF THE PERFORMANCES OF $\text{NH}_3\text{-H}_2\text{O}$ , $\text{NH}_3\text{-LiNO}_3$ AND $\text{NH}_3\text{-NaSCN}$ ABSORPTION REFRIGERATION SYSTEMS

DA-WEN SUN

Department of Agricultural and Food Engineering, University College Dublin, National University of Ireland, Earlsfort Terrace, Dublin 2, Republic of Ireland

(Received 16 July 1996)

**Abstract**—In recent years, research has been devoted to improvement of the performance of ammonia-water absorption refrigeration systems. In this study, thermodynamic analyses for ammonia-water, ammonia-lithium nitrate and ammonia-sodium thiocyanate cycles are performed. Detailed thermodynamic properties of these binary fluids are expressed in polynomial equations. The performances of these three cycles are compared. It is found that ammonia-lithium nitrate and ammonia-sodium thiocyanate cycles are suitable alternatives to ammonia-water absorption systems. The performance of the ammonia-sodium thiocyanate cycle is slightly better than that of the ammonia-lithium nitrate cycle. © 1997 Elsevier Science Ltd.

Absorption	Air conditioning	Ammonia-lithium nitrate	Ammonia-sodium thiocyanate
Ammonia-water	Aqua-ammonia	Computer simulation	Mathematical model
Refrigeration	Heat pump	$\text{NH}_3\text{-H}_2\text{O}$	$\text{NH}_3\text{-LiNO}_3$
			$\text{NH}_3\text{-NaSCN}$
			Optimisation

### NOTATION

$E$  = Effectiveness  
 $h$  = Enthalpy (kJ/kg)  
 $m$  = Mass flow rate (kg/s)  
 $P$  = Pressure (kPa)  
 $Q$  = Thermal energy (kW)  
 $X$  = Ammonia mass fraction in solution  
 $T$  = Temperature (K)

#### Greek

$v$  = Specific volume ( $\text{m}^3/\text{kg}$ )  
 $\rho$  = Density ( $\text{kg}/\text{m}^3$ )

#### Subscripts

a = Absorber  
c = Condenser  
e = Evaporator  
ex = Solution heat exchanger  
g = Generator  
l = Liquid  
me = Mechanical  
v = Vapour

### INTRODUCTION

Absorption refrigerator systems have attracted increasing research interests in recent years. Unlike mechanical vapour compression refrigerators, these systems cause no ozone depletion and reduce demand on electricity supply. Besides, heat powered systems could be superior to electricity powered systems in that they harness inexpensive waste heat, solar, biomass or geothermal energy sources for which the cost of supply is negligible in many cases. This makes heat powered refrigeration a viable and economic option [1-6].

The most common absorption systems are  $\text{H}_2\text{O-LiBr}$  and  $\text{NH}_3\text{-H}_2\text{O}$  cycles. The advantage for refrigerant  $\text{NH}_3$  is that it can evaporate at lower temperatures (i.e. from  $-10$  to  $0^\circ\text{C}$ ) compared to  $\text{H}_2\text{O}$  (i.e. from  $4$  to  $10^\circ\text{C}$ ). Therefore, for refrigeration, the  $\text{NH}_3\text{-H}_2\text{O}$  cycle is used. Research

has been performed for  $\text{NH}_3\text{-H}_2\text{O}$  systems theoretically [7–10] and experimentally [11, 12]. These studies show that the  $\text{NH}_3\text{-H}_2\text{O}$  system exhibits a relatively low COP. Efforts are being made to search for better refrigerant–absorbent pairs that can improve system performance. It is proposed that  $\text{NH}_3\text{-LiNO}_3$  and  $\text{NH}_3\text{-NaSCN}$  cycles can be alternatives to  $\text{NH}_3\text{-H}_2\text{O}$  systems [13, 14]. Therefore, in the present study, the comparisons of the performances of  $\text{NH}_3\text{-H}_2\text{O}$ ,  $\text{NH}_3\text{-LiNO}_3$  and  $\text{NH}_3\text{-NaSCN}$  absorption cycles are performed.

### CYCLE DESCRIPTION

Figure 1 illustrates the main components of the absorption refrigeration cycle. High-pressure liquid refrigerant (2) from the condenser passes into the evaporator (4) through an expansion valve (3) that reduces the pressure of the refrigerant to the low pressure existing in the evaporator. The liquid refrigerant (3) vaporises in the evaporator by absorbing heat from the material being cooled and the resulting low-pressure vapour (4) passes to the absorber, where it is absorbed by the strong solution coming from the generator (8) through an expansion valve (10), and forms the weak solution (5). The weak solution (5) is pumped to the generator pressure (7), and the refrigerant in it is boiled off in the generator. The remaining solution (8) flows back to the absorber and, thus, completes the cycle. By weak solution (strong solution) is meant that the ability of the solution to absorb the refrigerant vapour is weak (strong), according to the ASHRAE definition [15]. In order to improve system performance, a solution heat exchanger is included in the cycle. If the cycle operates on  $\text{NH}_3\text{-H}_2\text{O}$ , an analyser and a rectifier need to be added to remove water vapour from the refrigerant mixture leaving the generator before reaching the condenser. For the current study, it is assumed that the refrigerant vapour contains 100% ammonia for compatibility of the results for  $\text{NH}_3\text{-H}_2\text{O}$ ,  $\text{NH}_3\text{-LiNO}_3$  and  $\text{NH}_3\text{-NaSCN}$  cycles.

The system performance is measured by the coefficient of performance (COP):

$$\text{COP} = \frac{Q_c}{Q_g + W_{me}} \quad (1)$$

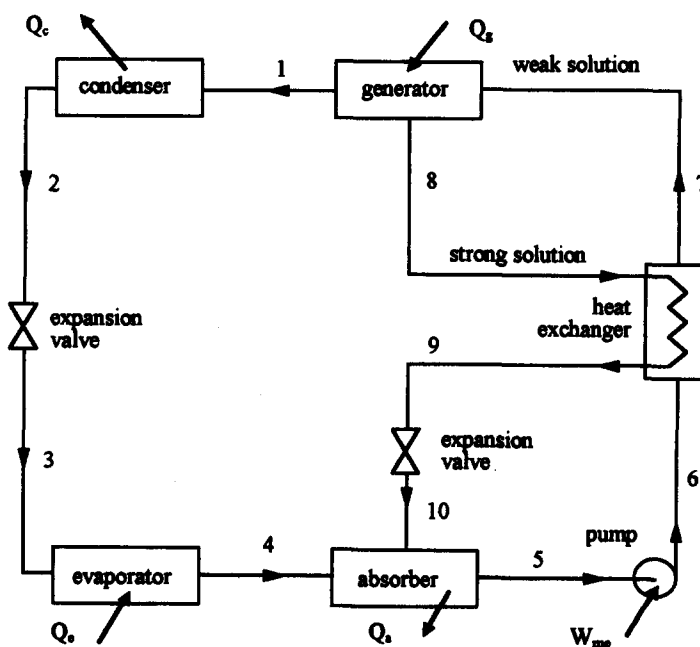


Fig. 1. The schematic of the absorption refrigeration cycle.

In order to use equation (1), mass and energy conservation should be determined at each component. For the generator, the mass and energy balances yield:

$$m_7 = m_1 + m_8 \text{ (total mass balance)} \quad (2)$$

$$m_7 X_7 = m_1 + m_8 X_8 \text{ (NH}_3 \text{ mass balance)} \quad (3)$$

$$Q_g = m_1 h_1 + m_8 h_8 - m_7 h_7 \quad (4)$$

From equations (2) and (3), the flow rates of the strong and weak solutions can be determined:

$$m_8 = \frac{1 - X_7}{X_7 - X_8} m_1 \quad (5)$$

$$m_7 = \frac{1 - X_8}{X_7 - X_8} m_1 \quad (6)$$

From equation (6), the circulation ratio of the system can be derived as

$$f = \frac{m_7}{m_1} \quad (7)$$

The energy balance for the solution heat exchanger is as follows:

$$T_9 = E_{ex} T_6 + (1 - E_{ex}) T_8 \quad (8)$$

$$h_7 = h_6 + \frac{m_8}{m_6} (h_8 - h_9) \quad (9)$$

The energy increase by pumping is

$$h_6 = h_5 + (P_6 - P_5) v_6 \quad (10)$$

$$W_{me} = (P_6 - P_5) v_6 \quad (11)$$

Finally, energy balances for the absorber, condenser and evaporator yield

$$Q_a = m_4 h_4 + m_{10} h_{10} - m_5 h_5 \quad (12)$$

$$Q_c = m_1 (h_1 - h_2) \quad (13)$$

$$Q_e = m_1 (h_4 - h_3) \quad (14)$$

If the generator, condenser, absorber and evaporator temperatures and the refrigerant mass flow rate or the required refrigerating load are given, the above equations can be solved simultaneously to give the system performance.

### THERMODYNAMIC PROPERTIES

For  $\text{NH}_3\text{-H}_2\text{O}$ ,  $\text{NH}_3\text{-LiNO}_3$  and  $\text{NH}_3\text{-NaSCN}$  absorption refrigeration cycles,  $\text{NH}_3$  is the refrigerant,  $\text{H}_2\text{O}$ ,  $\text{LiNO}_3$  and  $\text{NaSCN}$  are absorbents. The thermodynamic properties at states (1)–(4) in Fig. 1 are determined by  $\text{NH}_3$ , and other properties at states (5)–(10) can be calculated based on the binary mixture of  $\text{NH}_3\text{-H}_2\text{O}$ ,  $\text{NH}_3\text{-LiNO}_3$  or  $\text{NH}_3\text{-NaSCN}$  solutions.

#### Refrigerant $\text{NH}_3$

In the usual ranges of pressure and temperature concerning refrigeration applications, the two phase equilibrium pressure and temperature of the refrigerant  $\text{NH}_3$  are linked by the relation:

$$P(T) = 10^3 \sum_{i=0}^6 a_i (T - 273.15)^i \quad (15)$$

Table 1. Coefficients of equations (15)–(17)

<i>i</i>	<i>a<sub>i</sub></i> equation (15)	<i>b<sub>i</sub></i> equation (16)	<i>c<sub>i</sub></i> equation (17)
0	$4.2871 \times 10^{-1}$	$1.9879 \times 10^2$	$1.4633 \times 10^3$
1	$1.6001 \times 10^{-2}$	$4.4644 \times 10^0$	$1.2839 \times 10^0$
2	$2.3652 \times 10^{-4}$	$6.2790 \times 10^{-3}$	$-1.1501 \times 10^{-2}$
3	$1.6132 \times 10^{-6}$	$1.4591 \times 10^{-4}$	$-2.1523 \times 10^{-4}$
4	$2.4303 \times 10^{-9}$	$-1.5262 \times 10^{-6}$	$1.9055 \times 10^{-6}$
5	$-1.2494 \times 10^{-11}$	$-1.8069 \times 10^{-8}$	$2.5608 \times 10^{-8}$
6	$1.2741 \times 10^{-13}$	$1.9054 \times 10^{-10}$	$-2.5964 \times 10^{-10}$
Standard error	$1.6 \times 10^{-3}$	$8.5626 \times 10^0$	$1.059 \times 10^1$
Mean deviation	$1.252 \times 10^{-2}$	$5.566 \times 10^{-3}$	$3.679 \times 10^{-3}$

The specific enthalpies of saturated liquid and vapour NH<sub>3</sub> are expressed in terms of temperature as follows:

$$h_l(T) = \sum_{i=0}^6 b_i(T - 273.15)^i \tag{16}$$

$$h_v(T) = \sum_{i=0}^6 c_i(T - 273.15)^i \tag{17}$$

The above equations are fitted by the author with source data taken from the ASHRAE handbook [16]. Their coefficients are listed in Table 1.

*NH<sub>3</sub>-H<sub>2</sub>O solution*

The relation between saturation pressure and temperature of an ammonia–water mixture is given as [17]:

$$\log P = A - \frac{B}{T} \tag{18a}$$

where

$$A = 7.44 - 1.767X + 0.9823X^2 + 0.3627X^3 \tag{18b}$$

$$B = 2013.8 - 2155.7X + 1540.9X^2 - 194.7X^3 \tag{18c}$$

The relation among temperature, concentration and enthalpy is as follows, with coefficients given in Table 2 [18]:

$$h(T, \bar{X}) = 100 \sum_{i=1}^{16} a_i \left( \frac{T}{273.16} - 1 \right)^{m_i} \bar{X}^{n_i} \tag{19a}$$

where  $\bar{X}$  is the ammonia mole fraction and is given as follows:

$$\bar{X} = \frac{18.015X}{18.015X + 17.03(1 - X)} \tag{19b}$$

Table 2. Coefficients of equation (19)

<i>i</i>	<i>m<sub>i</sub></i>	<i>n<sub>i</sub></i>	<i>a<sub>i</sub></i>	<i>i</i>	<i>m<sub>i</sub></i>	<i>n<sub>i</sub></i>	<i>a<sub>i</sub></i>
1	0	1	$-7.61080 \times 10^0$	9	2	1	$2.84179 \times 10^0$
2	0	4	$2.56905 \times 10^1$	10	3	3	$7.41609 \times 10^0$
3	0	8	$-2.47092 \times 10^2$	11	5	3	$8.91844 \times 10^2$
4	0	9	$3.25952 \times 10^2$	12	5	4	$-1.61309 \times 10^3$
5	0	12	$-1.58854 \times 10^2$	13	5	5	$6.22106 \times 10^2$
6	0	14	$6.19084 \times 10^1$	14	6	2	$-2.07588 \times 10^2$
7	1	0	$1.14314 \times 10^1$	15	6	4	$-6.87393 \times 10^0$
8	1	1	$1.18157 \times 10^0$	16	8	0	$3.50716 \times 10^0$

Table 3. Coefficients of equation (20)\*

<i>i</i>	<i>j</i>	$a_{ij}$	<i>i</i>	<i>j</i>	$a_{ij}$	<i>i</i>	<i>j</i>	$a_{ij}$	<i>i</i>	<i>j</i>	$a_{ij}$
0	0	$9.9842 \times 10^{-4}$	0	1	$3.5489 \times 10^{-4}$	0	2	$-1.2006 \times 10^{-4}$	0	3	$3.2426 \times 10^{-4}$
1	0	$-7.8161 \times 10^{-8}$	1	1	$5.2261 \times 10^{-6}$	1	2	$-1.0567 \times 10^{-5}$	1	3	$9.8890 \times 10^{-6}$
2	0	$8.7601 \times 10^{-9}$	2	1	$-8.4137 \times 10^{-8}$	2	2	$2.4056 \times 10^{-7}$	2	3	$-1.8715 \times 10^{-7}$
3	0	$-3.9076 \times 10^{-11}$	3	1	$6.4816 \times 10^{-10}$	3	2	$-1.9851 \times 10^{-9}$	3	3	$1.7727 \times 10^{-9}$

\*Standard error =  $4.058 \times 10^{-6}$ , mean deviation =  $2.195 \times 10^{-3}$ .

The relation among specific volume, temperature and concentration is fitted by the author with source data taken from ASHRAE handbook [16] and is given as, with the fitted coefficients listed in Table 3:

$$v(T, X) = \sum_{j=0}^3 \sum_{i=0}^3 a_{ij}(T - 273.15)^i X^j \quad (20)$$

### $NH_3$ - $LiNO_3$ solution

The relation between saturation pressure and temperature of an ammonia-lithium nitrate mixture is given as [13]:

$$\ln P = A + \frac{B}{T} \quad (21a)$$

where

$$A = 16.29 + 3.859(1 - X)^3 \quad (21b)$$

$$B = -2802 - 4192(1 - X)^3 \quad (21c)$$

The relation among temperature, concentration and enthalpy is as follows [13]:

$$h(T, X) = A + B(T - 273.15) + C(T - 273.15)^2 + D(T - 273.15)^3 \quad (22a)$$

where

$$A = -215 + 1570(0.54 - X)^2 \quad \text{if } X \leq 0.54 \quad (22b)$$

$$A = -215 + 689(X - 0.54)^2 \quad \text{if } X \geq 0.54 \quad (22c)$$

$$B = 1.15125 + 3.382678X \quad (22d)$$

$$C = 10^{-3}(1.099 + 2.3965X) \quad (22e)$$

$$D = 10^{-5}(3.93333X) \quad (22f)$$

The solution density is related to concentration and temperature as [13]:

$$\rho(T, X) = 2046.222 - 1409.653\sqrt{X} - 1.3463(T - 273.15) - 0.0039(T - 273.15)^2 \quad (23)$$

### $NH_3$ - $NaSCN$ solution

The relation between saturation and temperature of an ammonia-sodium thiocyanate mixture is given as [13]:

$$\ln P = A + \frac{B}{T} \quad (24a)$$

where

$$A = 15.7266 - 0.298628X \quad (24b)$$

$$B = -2548.65 - 2621.92(1 - X)^3 \quad (24c)$$

The relation among temperature, concentration and enthalpy is as follows [13]:

$$h(T, X) = A + B(T - 273.15) + C(T - 273.15)^2 + D(T - 273.15)^3 \quad (25a)$$

where

$$A = 79.72 - 1072X + 1287.9X^2 - 295.67X^3 \quad (25b)$$

$$B = 2.4081 - 2.2814X + 7.9291X^2 - 3.5137X^3 \quad (25c)$$

$$C = 10^{-2}(1.255X - 4X^2 + 3.06X^3) \quad (25d)$$

$$D = 10^{-5}(-3.33X + 10X^2 - 3.33X^3) \quad (25e)$$

The solution density is related to concentration and temperature as [13]:

$$\rho(T, X) = A + B(T - 273.15) + C(T - 273.15)^2 \quad (26a)$$

where

$$A = 1707.519 - 2400.4348X + 2256.5083X^2 - 930.0637X^3 \quad (26b)$$

$$B = -3.6341X + 5.4552X^2 - 3.1674X^3 \quad (26c)$$

$$C = 10^{-3}(5.1X - 3.6X^2 - 5.4X^3) \quad (26d)$$

## RESULTS AND DISCUSSION

In order to compare the performance of ammonia–water, ammonia–lithium nitrate and ammonia–sodium thiocyanate absorption cycles, a computer simulation program was developed based on the above analyses, coupled with the thermodynamic property equations (15)–(26).

Table 4 shows the comparison of the various thermodynamic states in the cycle operating at  $T_g = 100^\circ\text{C}$ ,  $T_c = 30^\circ\text{C}$ ,  $T_a = 25^\circ\text{C}$  and  $T_e = -5^\circ\text{C}$ , with the effectiveness of the solution heat exchanger of 80%. Since ammonia is the refrigerant in these three cycles, high operating pressures are observed. The total solution amounts circulated are 3.56, 4.09 and 5.35 kg/min for  $\text{NH}_3\text{-H}_2\text{O}$ ,  $\text{NH}_3\text{-LiNO}_3$  and  $\text{NH}_3\text{-NaSCN}$ , respectively. This means that more refrigerant can be boiled off in the generator for the  $\text{NH}_3\text{-H}_2\text{O}$  cycle than for the other two. As a result, a bigger pump is needed for the  $\text{NH}_3\text{-NaSCN}$  cycle. Table 4 also shows that the thermodynamic properties for the three solutions are quite different, resulting in different energy flows to or from each component for these

Table 4. Thermodynamic properties at various states in ammonia–water, ammonia–lithium nitrate and ammonia–sodium thiocyanate cycles\*

Fluid state	$T(^{\circ}\text{C})$	$P(\text{kPa})$	$X(\%)$	$m(\text{kg}/\text{min})$	$h(\text{kJ}/\text{kg})$
$\text{NH}_3\text{-H}_2\text{O}$ cycle					
Generator ref exit (1)	100.00	1166.92	100.00	1.00	1448.44
Condenser ref exit (2)	30.00	1166.92	100.00	1.00	340.78
Evaporator ref exit (4)	-5.00	354.42	100.00	1.00	1456.62
Absorber sol exit (5)	25.00	354.42	52.24	3.56	-141.29
Generator sol inlet (7)	67.70	1166.92	52.24	3.56	59.46
Generator sol exit (8)	100.00	1166.92	33.55	2.56	223.37
Absorber sol inlet (10)	40.00	354.42	33.55	2.56	-54.55
$\text{NH}_3\text{-LiNO}_3$ cycle					
Generator ref exit (1)	100.00	1166.92	100.00	1.00	1448.44
Condenser ref exit (2)	30.00	1166.92	100.00	1.00	340.78
Evaporator ref exit (4)	-5.00	354.42	100.00	1.00	1456.62
Absorber sol exit (5)	25.00	354.42	53.51	4.09	-139.11
Generator sol inlet (7)	65.09	1166.92	53.51	4.09	-3.51
Generator sol exit (8)	100.00	1166.92	38.49	3.09	103.45
Absorber sol inlet (10)	40.00	354.42	38.49	3.09	-74.89
$\text{NH}_3\text{-NaSCN}$ cycle					
Generator ref exit (1)	100.00	1166.92	100.00	1.00	1448.44
Condenser ref exit (2)	30.00	1166.92	100.00	1.00	340.78
Evaporator ref exit (4)	-5.00	354.42	100.00	1.00	1456.62
Absorber sol exit (5)	25.00	354.42	49.12	5.35	-101.40
Generator sol inlet (7)	69.60	1166.92	49.12	5.35	25.13
Generator sol exit (8)	100.00	1166.92	37.43	4.35	98.26
Absorber sol inlet (10)	40.00	354.42	37.43	4.35	-56.27

\*ref = refrigerant, sol = solution, the number in brackets is shown in Fig. 1.

Table 5. Energy flow for each component in ammonia–water, ammonia–lithium nitrate and ammonia–sodium thiocyanate cycles

Energy flow	NH <sub>3</sub> –H <sub>2</sub> O	NH <sub>3</sub> –LiNO <sub>3</sub>	NH <sub>3</sub> –NaSCN
Generator $Q_g$ (kW)	30.1314	29.7138	29.0292
Condenser $Q_c$ (kW)	18.4611	18.4611	18.4611
Evaporator $Q_e$ (kW)	18.5974	18.5974	18.5974
Absorber $Q_a$ (kW)	30.3269	29.9067	29.2425
Pump $W_{mc}$ (kW)	0.0592	0.0566	0.0770
Recovery $Q_{ex}$ (kW)	11.8382	9.1952	11.2151
COP	0.6160	0.6247	0.6390

three cycles. This is illustrated in Table 5, in which the same operating conditions as in Table 4 are used. It can be seen from Table 5 that the main energy consumption occurs at the generator, and that the mechanical work required for the pump is very small and can be omitted for general calculations or when information on solution density is not available. Since the energy supplied to the evaporator is the same for these three cycles, the energy consumption at the generator determines the level of COP values. Table 5 shows that the COP value is the highest for the NH<sub>3</sub>–NaSCN cycle and the lowest for the NH<sub>3</sub>–H<sub>2</sub>O cycle. In Table 5, the importance of the solution heat exchanger for the heat recovery is also shown. Without heat recovery, the COP values would be much lower.

Figure 2 shows the comparison of COP values vs generator temperatures for NH<sub>3</sub>–H<sub>2</sub>O, NH<sub>3</sub>–LiNO<sub>3</sub> and NH<sub>3</sub>–NaSCN absorption cycles. The COP values for these three cycles increase with generator temperatures. There exists a low generator temperature limit for each cycle. Each cycle cannot be operated at generator temperatures lower than its limit. For the NH<sub>3</sub>–LiNO<sub>3</sub> cycle a lower generator temperature can be used than for the others. This is an important point for utilizing solar energy since fluid temperatures for flat plate solar collectors are generally below 90°C. It is shown that, for generator temperatures higher than 80°C, the NH<sub>3</sub>–NaSCN cycle gives the best performance, and the NH<sub>3</sub>–H<sub>2</sub>O cycle has the lowest COP. However, the differences among them are not very remarkable. For low generator temperatures, the NH<sub>3</sub>–LiNO<sub>3</sub> cycle gives the

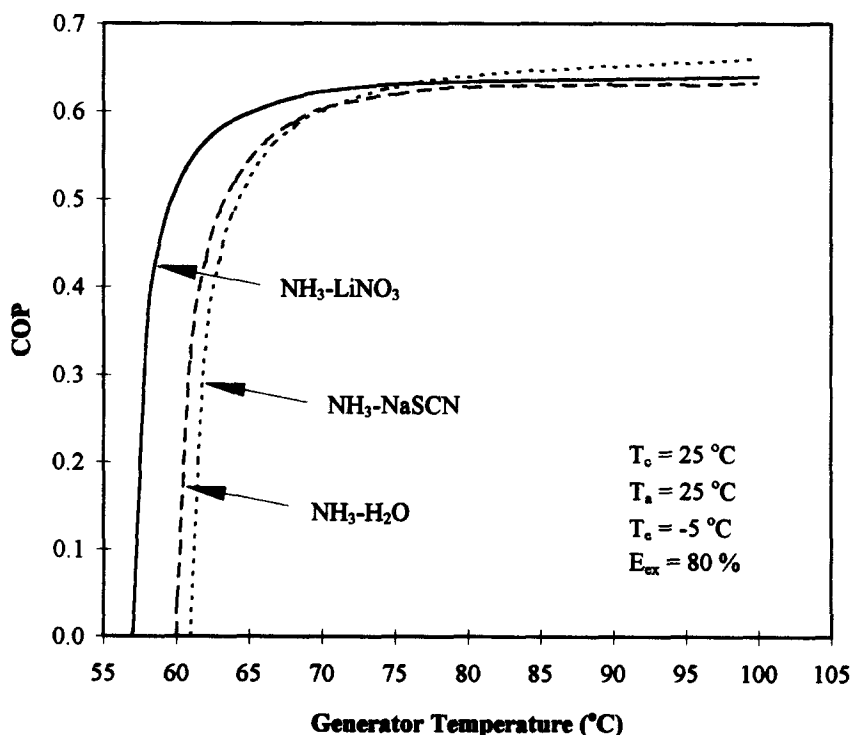


Fig. 2. Comparison of the effect of COP values on generator temperatures.

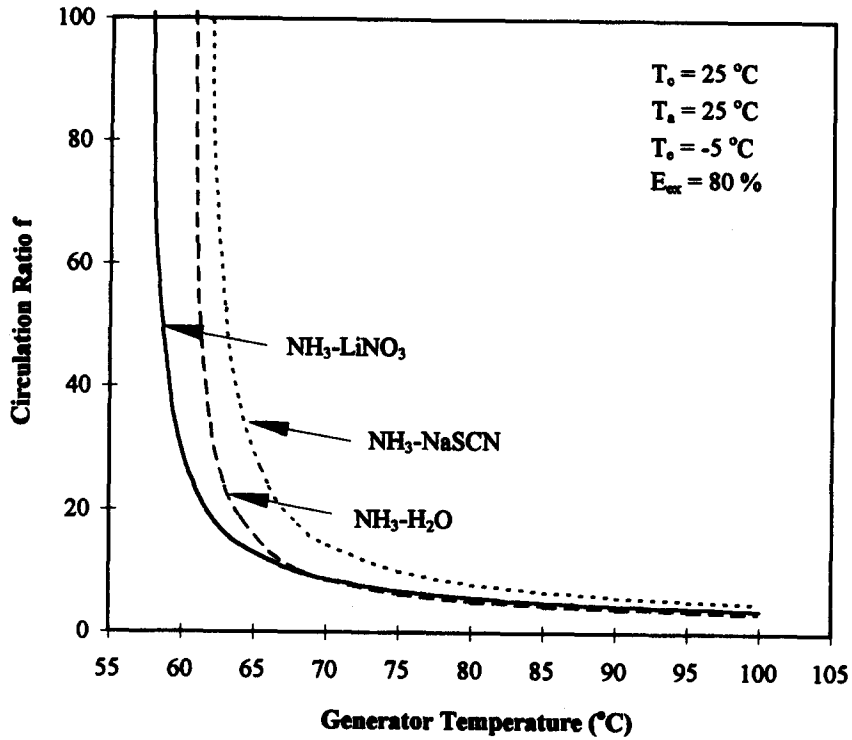


Fig. 3. Comparison of the effect of circulation ratio values on generator temperatures.

best performance. Figure 3 shows the corresponding comparison of circulation ratios vs generator temperatures. It is illustrated that the circulation ratio for the  $\text{NH}_3\text{-NaSCN}$  cycle is higher than for the other two cycles. This means that either the solution pump needs to run faster or a bigger

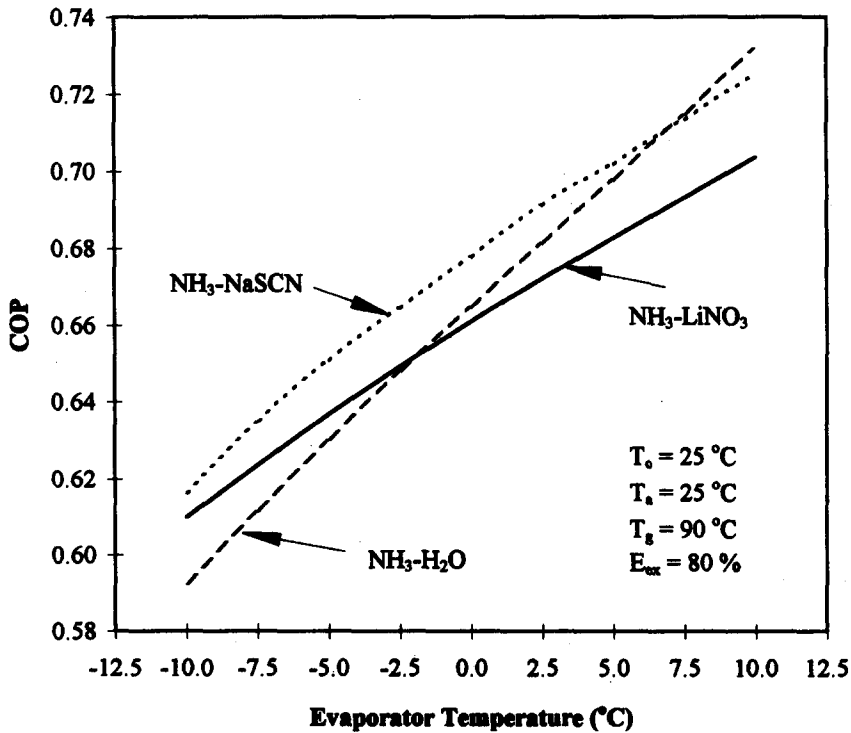


Fig. 4. Comparison of the effect of COP values on evaporator temperatures.

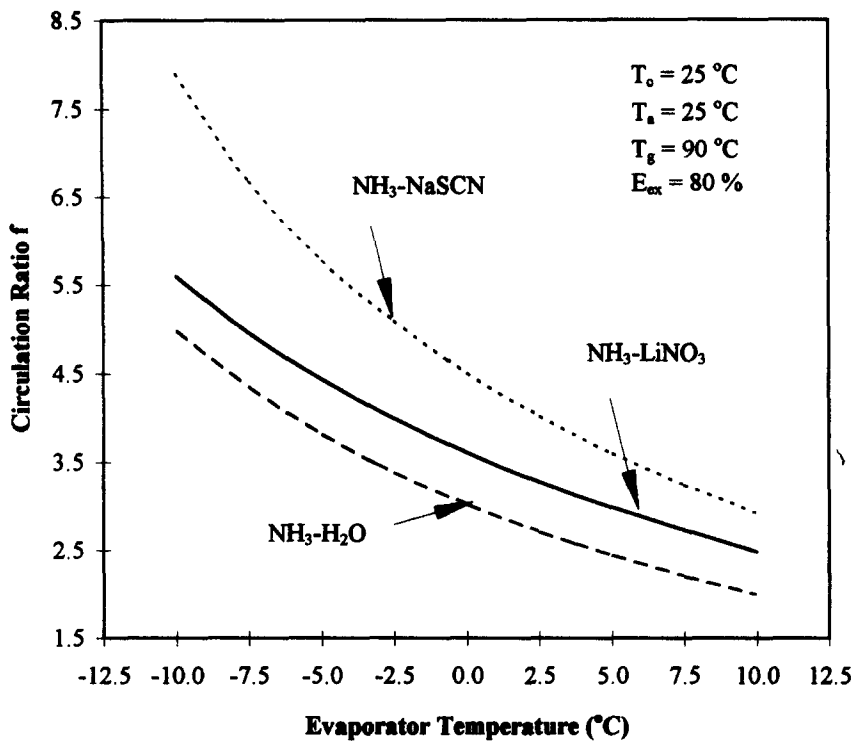


Fig. 5. Comparison of the effect of circulation ratio values on evaporator temperatures.

pump is required. If the generator temperature approaches its low temperature limit, the circulation ratio increases dramatically. Therefore, it is highly impractical to operate a cycle at a generator temperature too low, although it is still operable as shown in Figs 2 and 3.

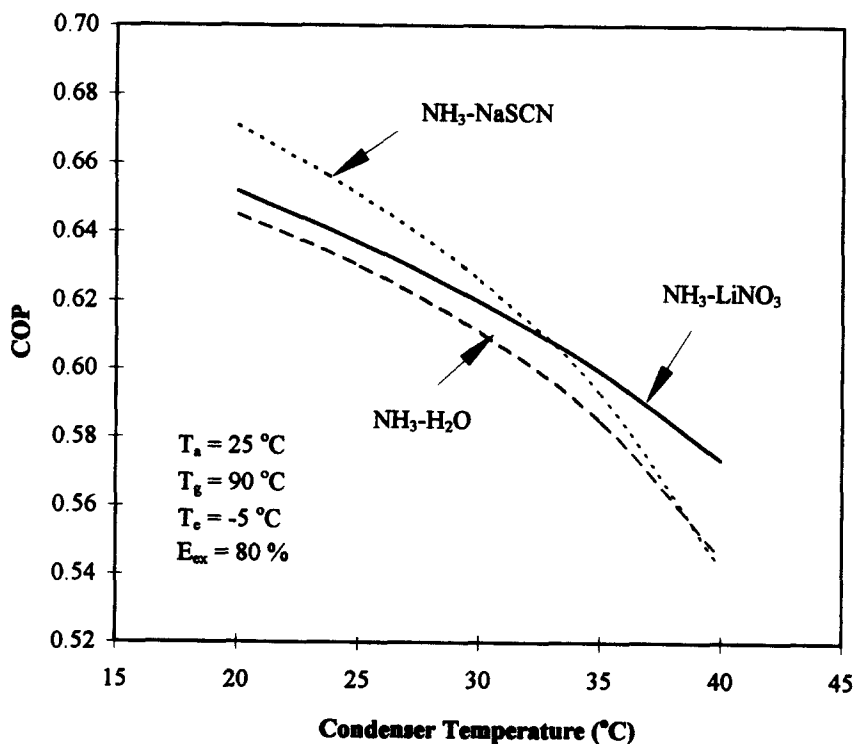


Fig. 6. Comparison of the effect of COP values on condenser temperatures.

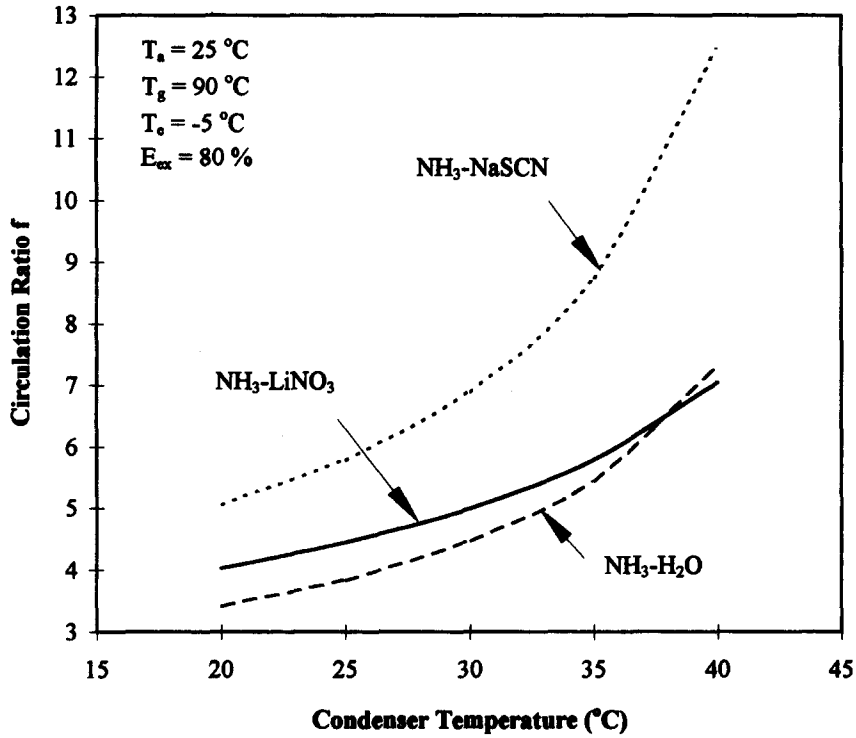


Fig. 7. Comparison of the effect of circulation ratio values on condenser temperatures.

Figure 4 gives the comparison of COP values vs evaporator temperatures for  $\text{NH}_3\text{-H}_2\text{O}$ ,  $\text{NH}_3\text{-LiNO}_3$  and  $\text{NH}_3\text{-NaSCN}$  absorption cycles. With the increase in evaporator temperature, the COP values for each cycle increase. For evaporator temperatures lower than zero, which is the

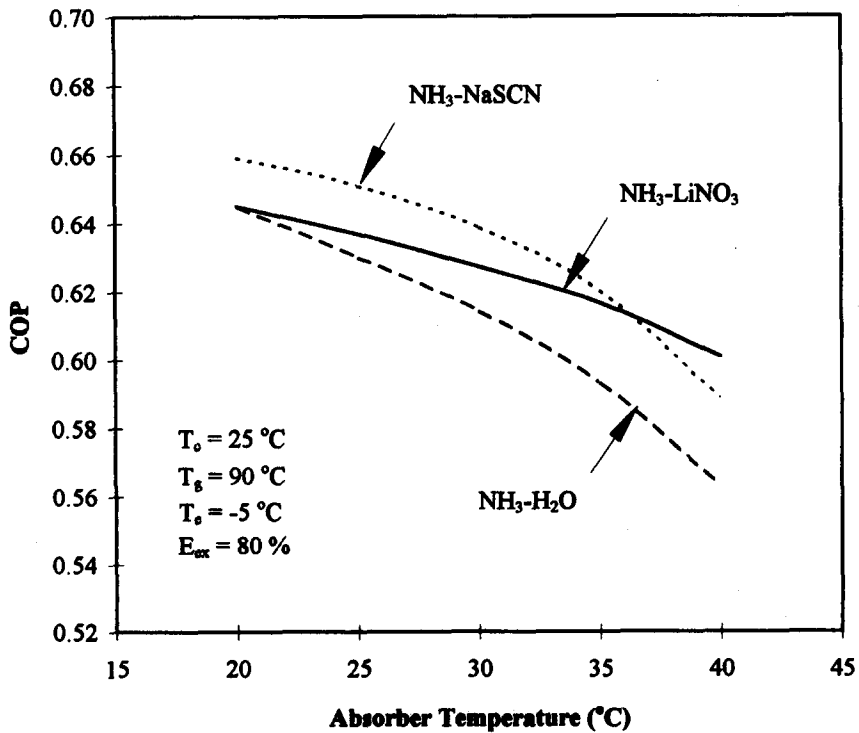


Fig. 8. Comparison of the effect of COP values on absorber temperatures.

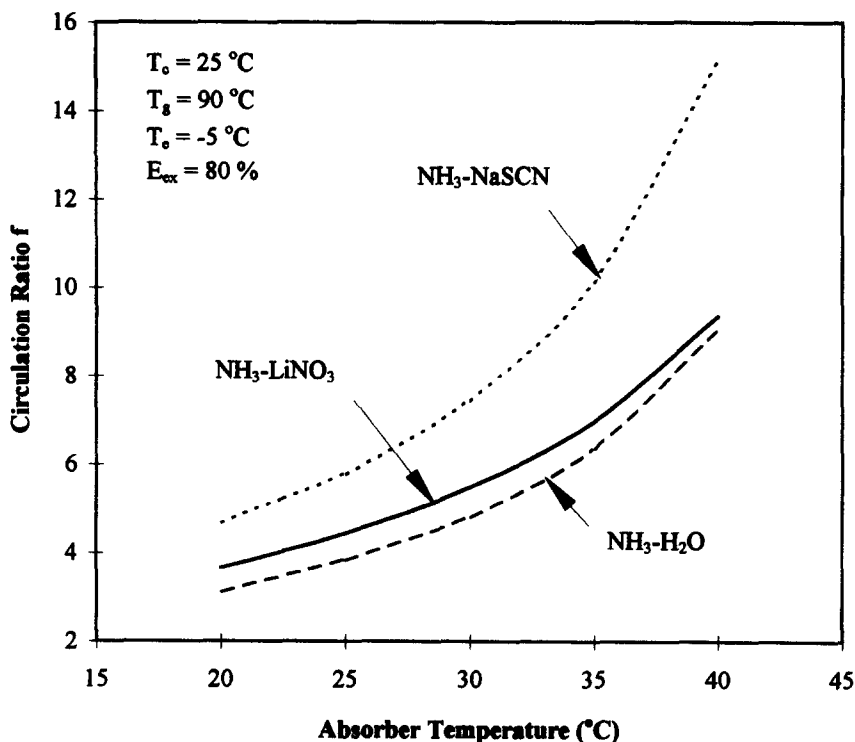


Fig. 9. Comparison of the effect of circulation ratio values on absorber temperatures.

temperature range for refrigeration, the  $\text{NH}_3\text{-NaSCN}$  cycle gives the best performance, and the  $\text{NH}_3\text{-H}_2\text{O}$  cycle has the lowest COP values. However, for high evaporator temperature, the performance of the  $\text{NH}_3\text{-H}_2\text{O}$  cycle is better than that of the  $\text{NH}_3\text{-LiNO}_3$  cycle. The corresponding comparison of circulation ratios vs evaporator temperatures is given in Fig. 5. Again, it is shown that the circulation ratio for the  $\text{NH}_3\text{-NaSCN}$  cycle is higher than the other two cycles. Figure 6 illustrates the comparison of COP values vs condenser temperatures for  $\text{NH}_3\text{-H}_2\text{O}$ ,  $\text{NH}_3\text{-LiNO}_3$ , and  $\text{NH}_3\text{-NaSCN}$  absorption cycles. Increasing condenser temperatures cause a decrease in system performance for each cycle. For condenser temperatures ranging from  $20^\circ\text{C}$  to  $40^\circ\text{C}$ , both the  $\text{NH}_3\text{-NaSCN}$  and  $\text{NH}_3\text{-LiNO}_3$  cycles show better performance than the  $\text{NH}_3\text{-H}_2\text{O}$  cycle. Figure 6 shows that, for low condenser temperatures, the COP values for the  $\text{NH}_3\text{-NaSCN}$  cycle are the highest, while for high condenser temperatures, the  $\text{NH}_3\text{-LiNO}_3$  cycle has the highest COP values. Figure 7 illustrates the corresponding comparison of circulation ratios vs condenser temperatures. The circulation ratio for the  $\text{NH}_3\text{-NaSCN}$  cycle is still higher than for the other two cycles.

The comparison of COP values vs absorber temperatures for  $\text{NH}_3\text{-H}_2\text{O}$ ,  $\text{NH}_3\text{-LiNO}_3$  and  $\text{NH}_3\text{-NaSCN}$  absorption cycles is shown in Fig. 8. The effect of absorber temperature is similar to that of condenser temperature. Generally speaking, the condenser and absorber temperatures should be at a similar level. The corresponding comparison of circulation ratios vs absorber temperatures is given in Fig. 9. The results of Figs 2-9 show that the system performance for the  $\text{NH}_3\text{-NaSCN}$  and  $\text{NH}_3\text{-LiNO}_3$  cycles is better than that for the  $\text{NH}_3\text{-H}_2\text{O}$  cycle, however the improvement is not very remarkable. Considering the fact that, for the  $\text{NH}_3\text{-NaSCN}$  and  $\text{NH}_3\text{-LiNO}_3$  cycles, no analysers and rectifiers are needed, these two cycles are suitable alternatives to the  $\text{NH}_3\text{-H}_2\text{O}$  cycle. The advantages for using the  $\text{NH}_3\text{-NaSCN}$  and  $\text{NH}_3\text{-LiNO}_3$  cycles are very similar, however, for the  $\text{NH}_3\text{-NaSCN}$  cycle, it cannot operate below  $-10^\circ\text{C}$  evaporator temperature because of the possibility of crystallization [13].

### CONCLUSIONS

Absorption refrigeration cycles have attracted increasing interest in recent years. The ammonia-water absorption cycle is mainly used for refrigeration temperatures below  $0^\circ\text{C}$ . Alternative refrigerant-absorption pairs are being developed for improving system performance.

In this study, ammonia–water, ammonia–lithium nitrate and ammonia–sodium thiocyanate absorption refrigeration cycles are analysed, with their thermodynamic properties expressed in polynomial equations. The performances of these three cycles against various generator, evaporator, condenser and absorber temperatures are compared. The results show that the ammonia–lithium nitrate and ammonia–sodium thiocyanate cycles give better performance than the ammonia–water cycle, not only because of higher COP values, but also because of no requirement for analysers and rectifiers. Therefore, they are suitable alternatives to the ammonia–water cycle. Generally speaking, the performance for the ammonia–lithium nitrate and ammonia–sodium thiocyanate cycles are similar, with the latter being slightly better than the former. However, the ammonia–sodium thiocyanate cycle cannot operate at evaporator temperatures below  $-10^{\circ}\text{C}$  for the possibility of crystallization.

#### REFERENCES

1. Eames, I. W., Aphornratana, S. and Sun, Da-Wen, *Heat Recovery Systems & CHP*, 1995, **15**, 711–721.
2. Sun, Da-Wen, Eames, I. W. and Aphornratana, S., *International Journal of Refrigeration*, 1996, **19**(3), 172–180.
3. Sun, Da-Wen and Eames, I. W., *International Journal of Energy Research* 1996, **20**, 871–885.
4. Sun, Da-Wen, *Energy Conversion Management*, 1997, **38**(5), 479–491.
5. Sun, Da-Wen, *Energy*, 1996, **21**(10), 919–929.
6. Sun, Da-Wen, *Energy Sources*, 1997, **19**(4), 349–367.
7. Rogdakis, E. D. and Antonopoulos, K. A., *Energy*, 1992, **17**(5), 477–484.
8. Bulgan, A. T., *Energy Conversion Management*, 1995, **36**(2), 135–143.
9. Sun, Da-Wen, *Energy Sources*, 1997, **19**(7).
10. Sun, Da-Wen, *Applied Thermal Engineering* 1996, **17**(3), 211–221.
11. Bogart, M., *Ammonia Absorption Refrigeration in Industrial Processes*. Gulf, Houston, TX, 1981.
12. Butz, D. and Stephan, K., *International Journal of Refrigeration*, 1989, **12**, 204–212.
13. Infante Ferreira, C. A., *Solar Energy*, 1984, **32**, 231–236.
14. Rogdakis, E. D. and Antonopoulos, K. A., *Heat Recovery Systems & CHP*, 1995, **15**(6), 591–599.
15. ASHRAE, *ASHRAE Handbook, Refrigeration Systems and Applications*, Chapter 40, p. 40.1. ASHRAE, 1791 Tullie Circle, N. E., Atlanta, GA 30329, 1994.
16. ASHRAE, *ASHRAE Handbook, Fundamentals*, Chapter 17, p. 17.45 & p. 17.81. ASHRAE, 1791 Tullie Circle, N.E., Atlanta, GA 30329, 1993.
17. Bourseau, P. and Bugarel, R., *International Journal of Refrigeration*, 1986, **9**, 206–214.
18. Patek, J. and Klomfar, J., *International Journal of Refrigeration*, 1995, **18**(4), 228–234.